Nanotechnology **20** (2009) 135601 (7pp) doi:10.1088/0957-4484/20/13/135601

Control of growth mechanisms and orientation in epitaxial Si nanowires grown by electron beam evaporation

A Irrera, E F Pecora and F Priolo

MATIS CNR-INFM, Via Santa Sofia 64, I-95123 Catania, Italy
and
Physics and Astronomy Department, University of Catania, Via Santa Sofia 64, I-95123 Catania, Italy

E-mail: francesco.priolo@ct.infn.it

Received 28 October 2008, in final form 21 December 2008
Published 11 March 2009
Online at stacks.iop.org/Nano/20/135601

Abstract

The growth mechanisms of epitaxial Si nanowires (NWs) grown by electron beam evaporation (EBE) and catalyzed through gold droplets are identified. NWs are seen to grow both from adsorbed Si atoms diffusing from the substrate and forming a dip around them, and from directly impinging atoms. The growth of a 2D planar layer competing with the axial growth of the NWs is also observed and the experimental parameters determining which of the two processes prevails are identified. NWs with (111), (100) and (110) orientation have been found and the growth rate is observed to have a strong orientation dependence, suggesting a microscopic growth mechanism based on the atomic ordering along (110) ledges onto (111)-oriented terraces. By properly changing the range of experimental conditions we demonstrate how it is possible to favor the axial growth of the NWs, define their length and control their crystallographic orientation.

(Some figures in this article are in colour only in the electronic version)

1. Introduction

Nowadays the challenge towards smaller and smaller microelectronic chips [1] requires the ability to overcome the limits of top-down approaches, especially related to lithography processes. An accurate control of the nanostructures with high reproducibility, no time-consuming processes and low-expense techniques is a very important feature for industrial applications. Major advantages are promised by bottom-up and self-assembling synthesis methods where, under specific conditions, atoms have the ability to organize themselves, with the final result to grow nanometer-size structures with very attractive properties.

In the last few years the scientific community has devoted increasing interest to materials showing quantum confinement effects. Semiconductor nanowires (NWs) represent a promising system because excitons will be confined in two directions. Both the electrical and optical properties are dramatically modified with respect to the bulk material, so they are suitable candidates to become the building blocks for future electronic devices [2–4], photovoltaic cells [5, 6], sensor applications [7] and efficient light sources [8, 9]. A great advantage of this system is the possibility to grow them via a self-assembling method developed since 1964 [10, 11], in which the vapor–liquid–solid (VLS) mechanism has been demonstrated as an efficient technique to obtain NWs by the use of a foreign catalytic element agent, usually a nanoparticle made of metal atoms. The catalyst promotes an axial growth under the metallic droplets if the substrate is maintained at a specific temperature able to form a liquid eutectic. Actually this technique gives the possibility to control the NWs' size, length, composition and crystalline quality, thus determining the optical and electrical properties. Nowadays it is possible to obtain NWs of very different materials like II–VI, III–V or group IV semiconductors, silica or ZnO.

At present silicon is the main semiconductor in the microelectronics field, so silicon NWs (Si NWs) have attracted much interest for the possibility to integrate them in CMOS

technology, growing them directly in their final position within a device. Some groups have reported Si NWs grown under different physical mechanisms (oxide-assisted growth [12] or the vapor–solid–solid VSS method [13]), but the VLS technique remained undoubtedly the most extensively used method to grow them. In this case gold is the most widely chosen catalyst due to the formation of an Au/Si eutectic at a very low temperature (363 °C). Si NWs grown through the VLS method have been obtained with many different synthesis techniques like chemical vapor deposition (CVD) [14–16], molecular beam epitaxy (MBE) [17, 18] and thermal evaporation [19, 20]. Electron beam evaporation (EBE) is a quite important physical method, as opposed to CVD, much less expensive than MBE, well diffused and, being a non-UHV technique, with a much higher throughput, which makes it interesting for industrial applications. Nevertheless, despite the huge literature on Si NWs, only a very few works appear in the literature on Si NWs grown by this technique [21, 22] and the mechanisms occurring during growth are unknown. In addition, while it is known that NWs with different crystallographic orientations can be grown [23], the growth rate orientation dependence has not been studied and ways to control the NW orientation are strongly sought for.

In this paper we study the basic physical mechanisms leading to the growth of single-crystal Si NWs grown by EBE. In particular, we show that adsorbed atoms diffusing from the substrate play an important role and the epitaxial NWs have a growth rate strongly dependent on their orientation, revealing a specific atomistic growth mechanism. The possibility to control NW length, growth rate and crystalline direction by varying the processing conditions is also proved and discussed.

2. Experimental details

The NWs studied in this work were prepared by electron beam evaporation (EBE) using high purity gold pellets and silicon ingots as sources. n-type Si(111) substrates were placed on a heated sample holder and the deposition rate was monitored *in situ* through a quartz microbalance placed close to the substrates. Samples were UV oxidized and then they were dipped in HF (5% diluted) to obtain an oxide-free silicon surface without surface contamination. The HF etching is essential because we do not observe any NW growth in the sample with a native SiO_2 layer. Samples were then located in the vacuum chamber of the evaporator and a 2 nm thick gold layer was evaporated on top of them at room temperature. After deposition, samples were annealed at 700 °C for 2 h to induce the continuous gold layer breaking and the formation of gold droplets on the substrate. During the subsequent Si evaporation the substrate temperature was fixed at 450, 480 or 510 °C. The filament current of the gun was maintained constant to ensure a silicon flux at the position of the substrate of 2.5×10^{14} atoms cm^{-2} s^{-1} for all samples. The pressure during the evaporation was about 1×10^{-7} mbar. Structural characterization was performed by using a field emission scanning electron microscope (Zeiss Supra 25). Statistical analysis was conducted by using the Gatan Digital Microscope software on several images for each sample.

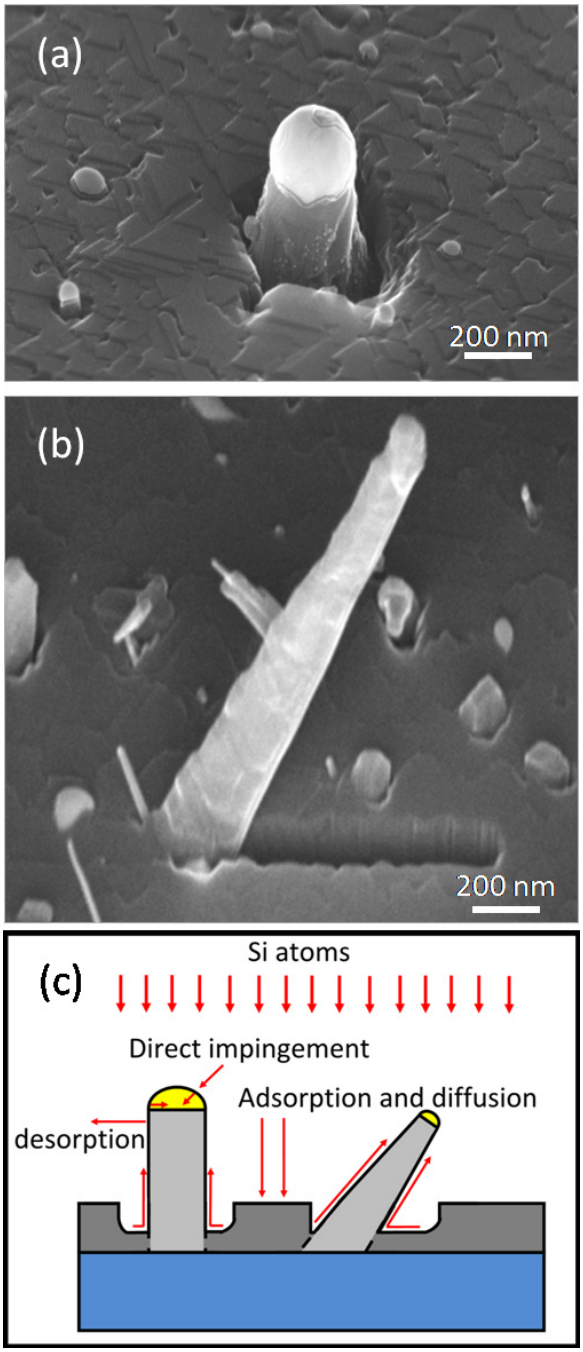

Figure 1. (a) SEM images of a cylindrical (111)-oriented well-shaped NW and (b) of an inclined (100)-oriented NW. Note in both cases the gold droplet on the top and the dip at the base. (c) Scheme of the proposed model for Si NW growth by EBE.

3. Results and discussion

3.1. Growth mechanisms

Typical Si NWs grown both perpendicular ((111) orientation) and inclined (in this case (100) orientation) with respect to the substrate are shown in the scanning electron microscopy (SEM) images in figures 1(a) and (b), respectively. The crystalline structure of the NWs can clearly be inferred by their perfect crystallographic orientation. In order to

further verify it, we have performed x-ray diffraction (XRD) measurements on several samples by using a Bruker AXS D5005 diffractometer using Cu Kα radiation with a grazing incidence angle of 0.5°. We have always observed the diffraction peaks relative to the Si substrate and Au clusters. A comparison with diffraction spectra of thin amorphous and polycrystalline Si layers suggests that in our NWs amorphous and/or polycrystalline components, if any, are negligible. It is quite striking to observe that, in spite of the non-UHV conditions, epitaxial NWs are obtained. NWs appear to be cylindrically shaped with a gold droplet on top. In particular the NW diameter is the same as the above standing droplet with no lateral or radial growth. In addition, a clear dip starting at the base of the NWs is present, indicating that adsorption and diffusion from the substrate are playing an important role in NW growth. The growth of NWs can be explained in terms of two competing processes: silicon atoms directly impinging on gold droplets and silicon atoms adsorbing on the substrate, as schematically depicted in figure 1(c). Silicon atoms impinging on gold droplets started to diffuse inside it causing a supersaturation of silicon until the conditions for the formation of the Au/Si eutectic are reached. At this point a liquid Au/Si alloy is formed and a layer-by-layer epitaxial silicon growth occurred just at the solid silicon/liquid eutectic interface under the gold droplet. This mechanism reflects the VLS principles and it is surely active in these samples as demonstrated by the gold droplet on top of the NWs. Atoms impinging on the substrate also have a fundamental role in the axial growth: in fact, the growth conditions allow them to easily diffuse over the sample in such a way that some of them can diffuse along the growing Si NW sidewalls. These atoms can be adsorbed just at the solid silicon/liquid eutectic interface under the gold droplet. Therefore they may have an important contribution to the NWs' growth. The existence of this mechanism is clearly demonstrated by the presence of a dip around the NWs, the atoms near the NWs acting as a sort of reservoir for the growth. This dip is usually not observed in NWs grown by conventional CVD because in that case we have only an axial growth thanks to the chemical catalytic effect of gold clusters on the surface. Due to the presence of the 2D growth, the NWs should be longer than they appear because a part of them is embedded in the 2D layer. This embedded part cannot show quantum confinement effects, so the electronic and optical properties are not influenced by it. Indeed, since the dip is completely surrounding the NW, we expect that the dip itself will also not influence the NW properties.

The behavior of atoms directly impinging on the gold cluster or reaching it from the substrate and then being incorporated can be considered similarly, because both of them contribute to the formation of the liquid eutectic under the droplet [18, 24].

Substrate temperature plays a key role because it determines the mean diffusion length of these atoms, and in particular their capability to epitaxially cover all the substrate or, in contrast, to agglomerate with the formation of silicon atoms cumuli. These atoms contributed also to a 2D silicon layer growth, that we experimentally measured, clearly competing with the NW axial growth. Note that for the inclined NW (figure 1(b)) the dip at the base is due in part also to a shadow effect which masks the deposition of the 2D layer. Moreover by increasing the substrate temperature the possibility to have Si atom desorption increases and the desorbed ad-atoms play a key role in the growth. Note that these processes occur at a silicon flux of $\sim 2.5 \times 10^{14}$ atoms cm^{-2} s^{-1}. At higher silicon fluxes we have not observed NW growth. This suggests that, if the silicon atoms flux impinging on the sample is too high, the 2D silicon deposition rate is faster than the silicon diffusion over the gold droplet and the subsequent epitaxial NW growth.

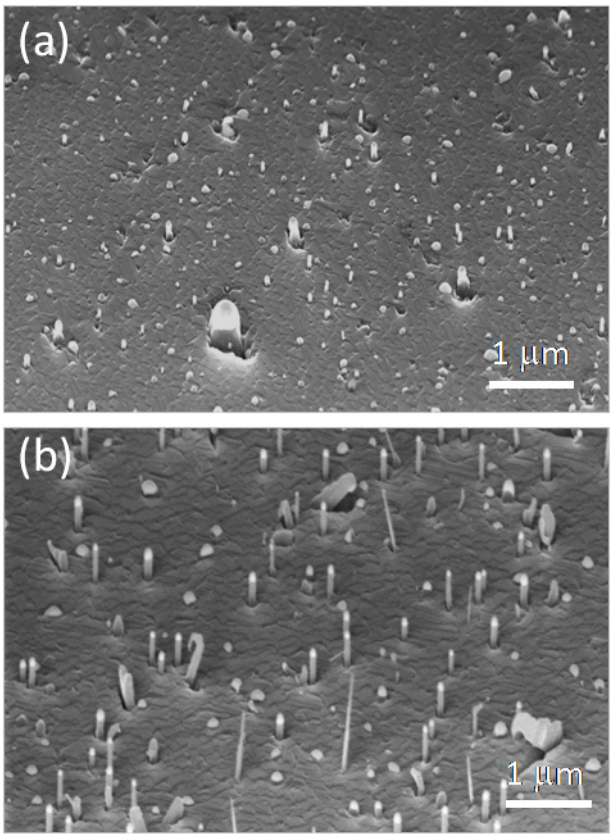

Figure 2. SEM images of NWs prepared with a substrate temperature of 480 °C and an evaporated silicon fluence of (a) 1.75×10^{18} atoms cm^{-2} and (b) 2×10^{18} atoms cm^{-2}.

With the gold droplet preparation being similar in all cases, the resulting NWs have comparable size under the different Si evaporations. We performed some attempts to grow silicon NWs starting from a sample with very small gold clusters (mean size of about 6 nm), but in this case we did not observe any NW growth. We consider this evidence related to the existence of a minimum radius for NW growth, mainly due to the Gibbs–Thompson effect.

3.2. Temperature dependence

Figure 2(a) shows an SEM image of a sample obtained with a substrate temperature of 480 °C and a silicon fluence of 1.75×10^{18} atoms cm^{-2}. We observed a few very short NWs with the gold droplet on top and many clear spots over the whole sample. We correlated them to gold droplets

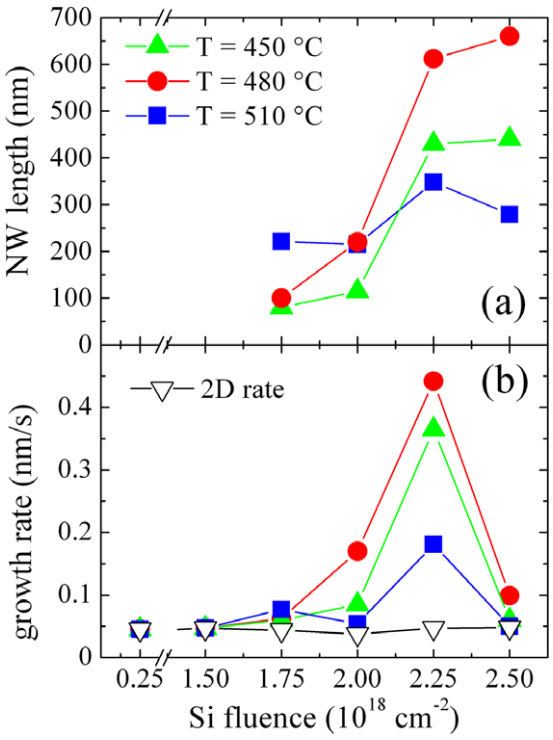

Figure 3. (a) Measured mean length of (111)-oriented NWs for samples grown at different temperatures. (b) 2D and axial rate values as a function of the evaporated silicon fluence for (111)-oriented NWs grown with substrate temperatures of 450, 480 and 510 °C.

which are catalyzing axial growth, but the NWs' length is still comparable with the 2D layer so we do not observe them outside the substrate. The situation dramatically changed by adding a further Si fluence of 0.25×10^{18} atoms cm^{-2}. In figure 2(b) the SEM image of a sample obtained with the same substrate temperature (480 °C) but with an Si fluence of 2×10^{18} atoms cm^{-2} is reported. In this sample we observed tall NWs emerging from the substrate, always with a clear gold droplet on top, thus confirming that VLS continued to be the basic growth mechanism.

Figure 3(a) reports an analysis of the (111)-oriented (vertical) NWs' length as a function of evaporated Si fluence for substrate temperatures of 450, 480 and 510 °C. It is very interesting to observe that, if the evaporated silicon fluence is below 1.75×10^{18} atoms cm^{-2}, we did not observe any NW growth at all temperatures. In other words, despite the fact that we had gold clusters on the substrate and many silicon atoms impinged on it, we had no catalyzed axial growth but only a layer-by-layer deposition covering the sample. It means that NW growth did not start immediately, and a temperature-independent 'incubation time' is needed before the 1D mechanism can begin, as known in the literature for NWs obtained by MBE and CVD techniques [18, 25, 26]. This is probably related to the time needed for the gold cluster to become saturated with Si and transform into a droplet. Indeed, it should be pointed out that, even if some axial growth occurred, if the NWs' length is less than the 2D layer thickness, it is not possible to observe them. Substrate temperature also plays an important role in the growth process. For 450 °C the NWs' mean length saturates to ∼400 nm for an evaporated Si fluence of 2.5×10^{18} atoms cm^{-2}. This NW maximum mean length increases to ∼660 nm for a deposition at 480 °C and it decreases again to ∼350 nm at 510 °C.

We described two different competing growth mechanisms in samples obtained by EBE: 2D layer and axial growth. It is very interesting to investigate which is the rate of these two processes to better understand the basic physical mechanism behind them. In particular the axial rate has to be higher than 2D growth when we observe NWs in the sample; vice versa 2D covering is predominant if the NWs in the sample are not observable. The axial rate can be obtained from a derivative of the data shown in figure 3(a), taking into account that the Si was deposited at a constant flux of about 2.5×10^{14} atoms cm^{-2} s^{-1}, as measured by the quartz microbalance. The 2D deposition rate was obtained by measuring in all samples the thickness of the 2D deposited layer by cross-sectional SEM and resulted in being constant at a value of ∼0.05 nm s^{-1}. These data are reported in figure 3(b). As described before, until a silicon fluence of 1.75×10^{18} atoms cm^{-2} we did not observe any NW growth. At the beginning axial growth was very slow, thus 2D covering was still predominating. Results changed for higher evaporated silicon fluence. Although the evaporating flux was always the same, we observed that NWs started to grow more quickly and, in fact, the axial rate continuously increased, reaching a maximum value of about 0.45 nm s^{-1}, which is about one order of magnitude higher than the 2D layer rate at a temperature of 480 °C. Axial growth needs an 'incubation time' to be initiated, but when it starts, it is very efficient for the presence of the gold as a catalyst and for the arrival of diffusing ad-atoms. At 450 and 510 °C the observed picture is similar but the rate is smaller in both cases than at 480 °C. In fact, at the lowest temperature the contribution of the diffusion of Si ad-atoms is negligible, as confirmed by the observation that the dip around the base of the NWs is absent. So at this temperature NWs grow mainly through the direct impingement of Si atoms. By increasing the temperature, the two temperature-activated competing processes, ad-atom diffusion (favoring growth) and atom desorption (limiting growth), occur. These are clearly demonstrated by the presence of the dip. It is possible to conclude that 480 °C is the optimal temperature for the fabrication of the longest NWs by EBE at the same growth conditions otherwise. Therefore at this temperature there is the best compromise between the diffusion of Si ad-atoms and their desorption. In contrast, at 510 °C the NW growth is limited, demonstrating that atom desorption from the surface is, in this regime, the most efficient process.

3.3. Orientation dependence

The discussion reported above regards perpendicular (111)-oriented NWs. However, we observed NWs both perpendicular and inclined and we will demonstrate that by controlling the experimental conditions of growth it is possible to control the NWs' growth direction. The angle formed between an NW and the substrate is directly related to the crystallographic orientation of the NWs. It is important to note that NWs showing a change in their direction during growth were not

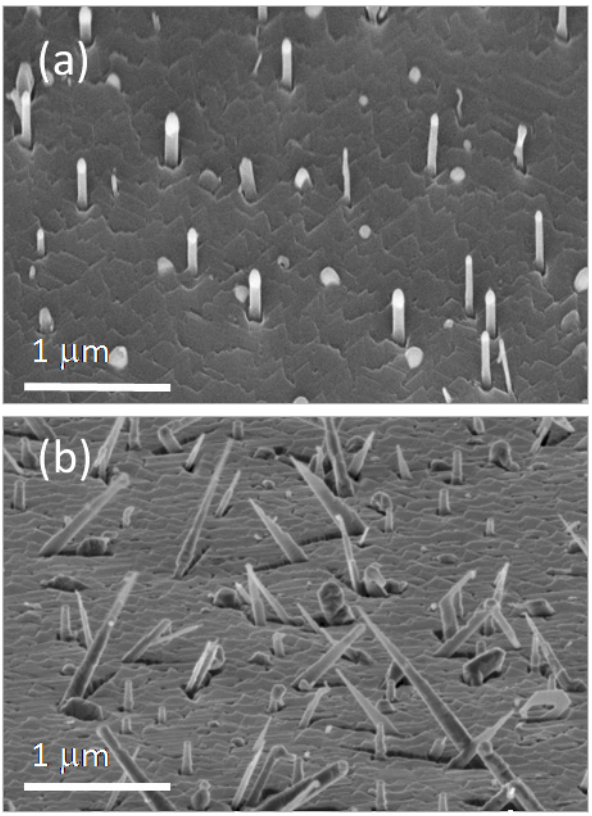

Figure 4. SEM images of samples prepared with a substrate temperature of 510 °C and an evaporated silicon fluence of (a) 2.0×10^{18} atoms cm^{-2} and (b) 2.50×10^{18} atoms cm^{-2}.

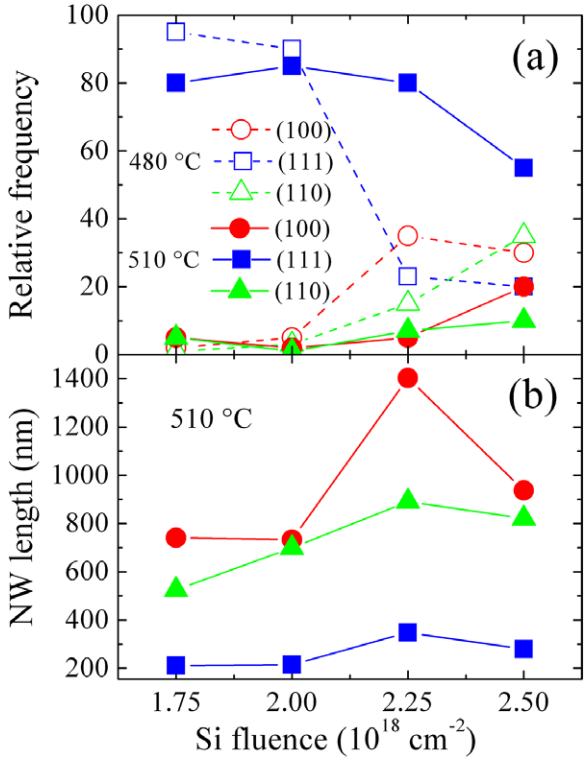

Figure 5. (a) Relative population for (111)-, (100)- and (110)-oriented NWs for NWs prepared with a substrate temperature of 480 and 510 °C. (b) NWs mean length as a function of the evaporated silicon fluence for (111)-, (100)- and (110)-oriented NWs grown at 510 °C.

present, different to what was reported for some cases of NWs obtained through the CVD technique [27]. It is direct evidence that EBE allows us to grow epitaxial NWs which are substantially defect-free. This result is similar to NWs obtained by MBE [28]. (100)-oriented NWs have a tilt angle with respect to the (111) substrate of 54°; (110)-oriented NWs at an angle of 45°; and (112)-oriented NWs at 74°.

The inclination angle between the substrate and the NW is commonly measured by controlling the tilt angle, tilting the sample and performing the SEM images [29, 30]. In fact, in this way it is possible to obtain a 3D perspective and to have a direct measure of the inclination of the NW. We measured the angle of each NW with respect to the substrate in all SEM images of properly tilted samples, so we were able to investigate the relative population and mean length of each crystallographic family. In this way we performed a detailed study with the aim of controlling the NWs' crystallographic directions by varying the experimental conditions. This is a very important capability because of the dependence of the electrical and optical properties on the crystallographic orientation [31, 32]. In this work, we show that by varying the experimental conditions it is possible to change the predominant relative percentage of the different NW orientations.

Figures 4 and 5 refer to the relative population and length of the different crystallographic families. In particular, figure 4(a) shows an SEM image of a sample in which all NWs are perpendicular to the substrate, i.e. (111)-oriented. This sample was prepared with a substrate temperature of 510 °C and an evaporated silicon fluence of 2×10^{18} atoms cm^{-2}. Figure 4(b) shows an SEM image of the sample prepared with a substrate temperature of 510 °C and an evaporated silicon fluence of 2.5×10^{18} atoms cm^{-2}. In this sample we observed NWs with different orientations, thus belonging to different crystallographic families and a lot of long inclined NWs are clearly present. Figure 5(a) reports the relative population for (111)-, (100)- and (110)-oriented NWs both for samples prepared with a substrate temperature of 480 and 510 °C as a function of the evaporated silicon fluence. We do not report statistics on the (112) family because we measured only a very few NWs with this orientation and only in some of the samples. This is a further demonstration of the absence of any SiO_2 layer because this orientation is favored in the presence of oxygen contamination [33]. In the graph a clear trend is observed, valid for both the substrate temperatures. At the beginning, after a silicon fluence of 1.75 or 2×10^{18} atoms cm^{-2}, substantially all of the NWs are perpendicular to the substrate, i.e. (111)-oriented, the relative population of this family being about 80–90%. By increasing the evaporated amount of silicon, the percentage of perpendicular NWs decreased (this is more evident for the lower substrate temperature), and (100)- or (110)-oriented NWs appeared. The percentage of (111)-oriented NWs can decrease to values as small as ∼20% for 480 °C growth at a fluence of 2.5×10^{18} atoms cm^{-2} while

the sum of (100)- and (110)-inclined NWs grows to values of ∼80% of the total population. Note that this decrease of the (111)-oriented NWs is facilitated also by the fact that, at high evaporated Si amounts, the growth rate of (111)-oriented NWs falls (figure 3(b)) and 2D covering starts suppressing the shortest NWs. By controlling the growth conditions it is hence possible to control the prevailing orientation. Indeed, (111)-oriented NWs always have a much smaller growth rate and remain somewhat short. On the other hand, (100) and (110) NWs appear at a later stage but grow much faster, becoming quite long. In fact, NWs longer than a micrometer are easily observed (see figure 4(b)). In other words, when the silicon amount reaching the sample is between 1.75 and -2×10^{18} atoms cm^{-2}, we do not have very tall NWs (about a few hundred nanometers) but they are always perpendicular to the substrate, while for geometrical reasons the inclined NWs are embedded in the 2D layer and so they are not visible. By continuing to evaporate silicon, the inclined NWs appear because they reach the length necessary to overcome the 2D layer while the shortest (111)-oriented NWs, due to a strong decrease in growth rate, remain embedded in the growing 2D layer. The combination of these two effects results in an increase in the percentage of inclined NWs. In order to quantify the growth rate and length as a function of crystallographic direction we measured the NWs' length in SEM images distinguishing their inclination and these data are reported in figure 5(b) as a function of the evaporated silicon fluence at a temperature of 510 °C. The trends are quite different: (100)-oriented NWs show a mean length up to 1400 nm, (110)-oriented NWs have a maximum mean length of about 900 nm and (111)-oriented NWs of ∼350 nm. In all cases the maximum length is reached after an evaporation of 2.25×10^{18} atoms cm^{-2}. It should be noted that the mean NW growth rate is twice as high for (100) with respect to (110) and four times as high for (100) with respect to (111).

The dependence of the growth rate with orientation is a very important result, because it is strictly related to the microscopic mechanism of growth. The existence of an orientation dependence in the growth rate strongly reminds us of the epitaxial recrystallization of amorphous Si layers. Moreover, even the trend of the rate as a function of the crystallographic orientation is the same as the well-known trend reported in the literature in the case of solid phase epitaxy processes [34]. It allows us to conclude that the microscopic mechanisms of growth might be similar. In particular in that case the growing crystal–amorphous interface minimizes its energy by forming (111)-oriented terraces connected through (110)-oriented ledges. The epitaxial growth occurs through atomic ordering along the (110) ledges that are maximum for the (100) orientation, decrease for the (110) orientation and are in principle zero for the exact (111) orientation. This results in the well-known orientation dependence of the amorphous silicon growth rate [34] and it can be easily adapted to the case of 1D NW growth because ledges and terraces have typical dimensions (a few nanometers) much smaller than the growing NW diameter, so the droplet diameter is larger than the surface which is crystallizing and it behaves as a planar substrate. The present data suggest that epitaxial ordering along (110) ledges onto (111)-oriented terraces is probably also the main microscopic atomistic growth mechanism for the growth of epitaxial Si NWs.

4. Conclusions

In conclusion, we have demonstrated the growth of epitaxial Si NWs by EBE under non-UHV conditions. The NW growth results from both ad-atoms diffusing from the substrate and atoms directly impinging on the gold droplet. The axial NW growth necessitates a temperature-independent 'incubation time' and competes with a 2D planar growth. We have conducted statistical analysis on the NWs' mean length, thus finding an optimum silicon fluence to obtain taller NWs. Lower silicon fluences are not useful because of an 'incubation time' before NW growth started; in contrast, NW growth seemed to saturate at high fluences. Also the substrate temperature plays a key role because the silicon mean diffusion length over the substrate is an energy-activated process which contributes to NW growth. At the same time, by increasing substrate temperature the desorption of the Si ad-atoms increases and therefore they cannot participate in the growth. This result in an optimum substrate given by a balance between the two competing effects.

NWs' crystallographic direction is a very important structural feature and we have demonstrated that it is possible to control their orientation by varying the experimental parameters. In particular, we have shown that, while at the beginning of the growth most NWs are (111)-oriented, at high Si fluences most of them are (100)- or (110)-oriented.

In conclusion, due to the different growth rates of the different orientations and to the presence of the 2D layer we are able to obtain samples with fixed percentages of (111)-, (100)- and (110)-oriented NWs. We have observed that the NW growth rate is strongly orientation-dependent, suggesting a microscopic atomistic growth mechanism based on epitaxial ordering along (110) ledges onto (111) terraces.

We have demonstrated that EBE is a growth technique that has great potentialities for Si NWs. The main advantage of using EBE as a growth technique is the possibility to obtain Si NWs epitaxial with the substrate. Moreover it is cheaper than MBE and we demonstrated that it allows an accurate control of the growth mechanisms and structural properties in non-UHV conditions. In fact, by properly varying the experimental parameters it is possible to define the length and crystallographic orientations of the NWs that are critical characteristics for a direct application in nanoelectronics. As a drawback, evaporation has to be performed with a very low rate to obtain high quality NWs, while by CVD it is possible to use very high rates for massive growth of NWs but these high rates, however, may result in poor crystalline quality.

Acknowledgments

The authors thank Fabio Iacona for useful discussions, Riccardo De Bastiani for XRD measurements and Carmelo Percolla for expert technical assistance.

References

[1] http://www.itrs.net
[2] Duan X, Huang Y, Cui Y, Wang J and Lieber C M 2001 *Nature* **409** 6816
[3] Cui Y, Zhong Z, Wang D, Wang W U and Lieber C M 2003 *Nano Lett.* **3** 149
[4] Thelander C *et al* 2006 *Mater. Today* **10** 28
[5] Tian B, Zheng X, Kempa T J, Fang Y, Yu N, Yu G, Huang J and Lieber C M 2007 *Nature* **449** 885
[6] Kayes B M, Atwater H A and Lewis N S 2005 *J. Appl. Phys.* **97** 114302
[7] Zhou X T, Hu J Q, Li C P, Ma D D, Lee C S and Lee S T 2003 *Chem. Phys. Lett.* **369** 220
[8] Huang M H, Mao S, Feick H, Yan H, Wu Y, Kind H, Weber E, Russo R and Yang P 2001 *Science* **292** 1897
[9] Qian F, Gradecak S, Li Y, Wen C Y and Lieber C M 2005 *Nano Lett.* **5** 2287
[10] Wagner R S and Ellis W C 1964 *Appl. Phys. Lett.* **4** 89
[11] Givargizov E I and Sheftal N N 1971 *J. Cryst. Growth* **9** 326
[12] Wang N, Tang Y H, Zhang Y F, Lee C S and Lee S T 1998 *Phys. Rev.* B **58** R16024
[13] Wang Y, Schmidt V, Senz S and Gösele U 2006 *Nat. Nanotechnol.* **1** 186
[14] Kamins T I, Williams R S, Basile D B, Hesjedal T and Harris J S 2001 *J. Appl. Phys.* **89** 1008
[15] Stelzner T, Andra G, Wendler E, Wesch W, Scholz R, Gösele U and Christiansen S 2006 *Nanotechnology* **17** 2895
[16] Iacopi F, Vereecken P M, Schaekers M, Caymax M, Moelans N, Blanpain B, Richard O, Detavernier C and Griffiths H 2007 *Nanotechnology* **18** 505307
[17] Schubert L, Werner P, Zakharov N D, Gerth G, Kolb F M, Long L and Gösele G 2004 *Appl. Phys. Lett.* **84** 4968
[18] Werner P, Zakharov N D, Gerth G, Schubert L and Gösele G 2006 *Int. J. Mater. Res.* **97** 1008
[19] Pan Z W, Dai Z R, Xu L, Lee S T and Wang Z L 2001 *J. Phys. Chem.* B **105** 2507
[20] Pan H, Lim S, Poh C, Sun H, Wu X, Feng Y and Lin J 2005 *Nanotechnology* **16** 417
[21] Sivakov V, Andra G, Himcinschi C, Gösele U, Zhan D R T and Christiansen S 2006 *Appl. Phys.* A **85** 311
[22] Sivakov V, Heyroth F, Falk F, Andra G and Christiansen S 2007 *J. Cryst. Growth* **300** 288
[23] Schmidt V, Senz S and Gösele U 2005 *Nano Lett.* **5** 931
[24] Dubrovskii V G, Sibirev N V, Cirlin G E, Harmand J C and Ustinov V M 2006 *Phys. Rev.* E **73** 021603
[25] Kalache B, Cabarrocas P R and Morral A F 2006 *Japan. J. Appl. Phys.* **45** L190
[26] Clement T, Ingole S, Ketharanathan S, Drucker J and Picraux S T 2006 *Appl. Phys. Lett.* **89** 163125
[27] Hofmann S, Ducati C, Neill R J, Piscanec S, Ferrari A C, Geng J, Dunin-Borkowski R E and Robertson J 2003 *J. Appl. Phys.* **94** 6005
[28] Zakharov N, Werner P, Sokolov L and Gösele U 2007 *Physica* E **37** 148
[29] Lugstein A, Steinmair M, Hyun Y J, Hauer G, Pongratz P and Bertagnolli E 2008 *Nano Lett.* **8** 2310
[30] Jagannathan H, Deal M, Nishi Y, Woodruff J, Chidsey C and McIntyre P C 2006 *J. Appl. Phys.* **100** 024318
[31] Zhao X, Wei C M, Yang L and Chou M Y 2004 *Phys. Rev. Lett.* **92** 236805
[32] Yan J, Yang L and Chou M Y 2007 *Phys. Rev.* B **76** 115319
[33] Tan T Y, Lee S T and Gosele U 2002 *Appl. Phys.* A **74** 423
[34] Csepregi L, Kennedy E F, Mayer J W and Sigmon T W 1978 *J. Appl. Phys.* **49** 3906